ResearchGate

See discussions, stats, and author profiles for this publication at: https://www.researchgate.net/publication/231691851

# Local orientational motions in flexible polymeric chains

**ARTICLE** *in* MACROMOLECULES · JULY 1990

Impact Factor: 5.8 · DOI: 10.1021/ma00206a041

CITATIONS
7

READS
10

**3 AUTHORS**, INCLUDING:

Ivet Bahar
University of Pittsburgh
**305** PUBLICATIONS **12,310** CITATIONS
SEE PROFILE

Burak Erman
Koc University
**220** PUBLICATIONS **5,963** CITATIONS
SEE PROFILE

Available from: Ivet Bahar
Retrieved on: 26 January 2016

and analyze the data in a similar way in order examine the relationship between the respective relaxation time distributions. Such studies have been initiated.

Measurements of the relaxation time distributions as a function of solvent quality show that the relative amplitudes of the slow modes decrease with increasing solvent quality and thus increasing thermodynamic interactions, but they remain observable even for good solvents.

## References and Notes


(1) de Gennes, P.-G. *Macromolecules* **1976**, *9*, 587, 594.
(2) de Gennes, P.-G. *Scaling Concepts in Polymer Physics*; Cornell University Press: London, 1979.
(3) Doi, M.; Edwards, S. F. *The Theory of Polymer Dynamics*; Oxford University Press: Oxford, 1986.
(4) Stepanek, P.; Konak, C. *Adv. Colloid Interface Sci.* **1984**, *21*, 195.
(5) Chu, B.; Nose, T. *Macromolecules* **1979**, *12*, 590, 599.
(6) Amis, E. J.; Han, C. C.; Matsushita, Y. *Polymer* **1984**, *25*, 650.
(7) Takahashi, M.; Nose, T. *Polymer* **1986**, *27*, 1071.
(8) Adam, M.; Delsanti, M. *J. Phys. (Paris) Lett.* **1984**, *45*, L-279.
(9) Adam, M.; Delsanti, M. *Macromolecules* **1985**, *18*, 1760.
(10) Brown, W. *Macromolecules* **1986**, *19*, 387, 1083.
(11) Brown, W.; Johnsen, R. M. *Macromolecules* **1986**, *19*, 2002.
(12) Brown, W.; Stepanek, P. *Macromolecules* **1988**, *21*, 1791.
(13) Brown, W.; Johnsen, R. M.; Stepanek, P.; Jakes, J. *Macromolecules* **1988**, *21*, 2859.
(14) Stepanek, P.; Konak, C.; Jakes, J. *Polym. Bull.* **1986**, *16*, 67.
(15) Stepanek, P.; Jakes, J.; Hrouz, J.; Brown, W. In *Polymer Motion in Dense Systems*; Richter, D., Springer, T., Eds.; Springer Proceedings in Physics, 1988; Vol. 198, p 29.
(16) Brochard, F.; de Gennes, P.-G. *Macromolecules* **1977**, *10*, 1157.
(17) Brochard, F. *J. Phys. (Paris)* **1983**, *44*, 39.
(18) Rouse, P. E. *J. Chem. Phys.* **1953**, *21*, 1272.
(19) Zimm, B. H. *J. Chem. Phys.* **1956**, *24*, 269.
(20) Pecora, R. *J. Chem. Phys.* **1965**, *43*, 1562.
(21) Yamakawa, H. *Modern Theory of Polymer Solutions*; Harper&Row: New York, 1974.
(22) Jakes, J., unpublished results.
(23) Provencher, S. W. *Makromol. Chem.* **1979**, *180*, 247.
(24) Livesey, A. K.; Delaye, M.; Licinio, P.; Brochon, J. E. *Faraday Discuss. Chem. Soc.* **1987**, *83*, 247.
(25) Livesey, A. K.; Delaye, M.; Licinio, P. *J. Chem. Phys.* **1986**, *84*, 5102.
(26) Jakes, J. *Czech. J. Phys. B* **1988**.
(27) Nicolai, T.; Brown, W.; Johnsen, R. M. *Macromolecules* **1989**, *22*, 2795. press.
(28) Geisler, E.; Hecht, A. M. *J. Phys. Lett.* **1979**, *40*, L-173.
(29) Ferry, J. D. *Viscoelastic Properties of Polymers*, 3rd ed.; Wiley: New York, 1980.
(30) Roots, J.,; Nyström, B. *Macromolecules* **1980**, *13*, 1595.
(31) Raju, V. R.; Menezes, E. V.; Marin, G.; Graessley, W. W., Fetters, L. J. *Macromolecules* **1981**, *14*, 1668.
(32) Wang, C. H.; Fisher, E. W. *J. Chem. Phys.* **1985**, *82*, 632.
(33) Wang, C. H.; Fisher, E. W. *J. Chem. Phys.* **1985**, *82*, 4332.
(34) Adam, M.; Delsanti, M. *J. Phys. (Les Ulis, Fr.)* **1983**, *44*, 1185.
(35) Adam, M.; Delsanti, M. *J. Phys. (Les Ulis, Fr.)* **1984**, *45*, 1513.
(36) Osaki, K.; Nishizawa, K.; Kurata, K. *Macromolecules* **1982**, *15*, 1068.
(37) Takahashi, Y.; Noda, I.; Nagasawa, M. *Macromolecules* **1985**, *18*, 2220.
(38) Takahashi, Y.; Umeda, M.; Noda, I. *Macromolecules* **1988**, *21*, 2257.
(39) *Base line* taken to equal the total number of counts times the number of counts per second.
(40) **Note Added in Proof**. It cannot be ruled out, however, that the split-up of the slow part of the decay time distribution is not artifactual and derives from modulation of the experimental correlogram by a small amount of systematic noise. A subsequent communication will deal with application of the generalized exponential distribution (GEX) to describe the total of all the slow components as an alternative procedure.


**Registry No.** Polystyrene, 9003-53-6.

# Local Orientational Motions in Flexible Polymeric Chains


**Ivet Bahar* and Burak Erman**

*Polymer Research Center and School of Engineering, Bogazici University, Bebek 80815, Istanbul, Turkey*

**Lucien Monnerie**

*Laboratoire de Physico-Chimie Structurale et Macromoléculaire, associé au C.N.R.S., 10, rue Vauquelin, 75 231 Paris Cedex 05, France.*

*Received March 24, 1989; Revised Manuscript Received July 26, 1989*


ABSTRACT: Effects of chain connectivity, viscous resistance of the environment, and internal barriers to conformational transitions are studied in relation to local orientational motions in flexible chains. Calculations are performed according to the dynamic rotational isomeric states scheme. Only a single transition over a bond at a time is assumed. That such single bond rotations are indeed possible in a sequence of 20 bonds without significant distortion of the tails is shown by the present analysis. The increase in the frictional resistance to motion with the size of the mobile sequence is investigated for polyethylene at 300 K. The latter, referred to as the size effect, is included in the treatment through consideration of the total path traveled by each of the moving atoms. Orientational autocorrelation functions for a bond at the end of an $N$ bond mobile sequence are evaluated in the presence and absence of the size effect. Two different correlation times, emphasizing short and long time motions, are defined. Dependence of the correlation times on the length of the mobile sequence is evaluated.


## Introduction

Long- and short-wavelength motions in a single polymer chain are controlled by three major factors: (i) the external resistance to motion exerted by the environmental frictional forces; (ii) the internal resistance associated with barriers to conformational transitions; (iii) the chain connectivity.

The first two factors are common to both small molecules and macromolecules. The third is an inherent property of macromolecules uniquely and distinguishes them

0024-9297/90/2223-1174$02.50/0 © 1990 American Chemical Society

from small molecules. Chain connectivity operates on both local and larger scales. On a local scale, intramolecular elastic forces operating on every skeletal atom impose restrictions on the types of orientational motions. On a larger scale, a given sequence of bonds in motion also experiences intramolecular forces at both ends as commonly represented by the bead-and-spring model. Those forces are stronger for more extended configurations in which the longer molecular dimensions are compatible with a smaller number of available transitions.

The effect of the first factor, the external resistance, is twofold. First, a frictional resistance operates all along the moving segment. A second effect is closely associated with chain connectivity and operates at the ends of the sequence in motion. Helfand classifies the types of local motions into three groups.[1] The first leaves the tails of the mobile group unchanged. Such crankshaft-like motions[2] require simultaneous rotations of two skeletal bonds and hence are opposed by stronger internal effects. A more probable class of motions is referred to as type 2 motions.[1] These motions are characterized by the fact that they lead only to translation of the tails. The third type of motion necessitates large swinging of the tails and is the least probable from an energetic point of view, as expected.

As to the internal barriers to motion, they originate from short-range intramolecular interaction and depend on the specific chemical and stereochemical structure and on the particular isomeric transition. de Gennes points out[3] that, in contrast to external effects, which increase with the size of the moving segment, the strength of internal resistance diminishes as a longer sequence of bonds is allowed to undergo orientational motion, as first discussed by Kuhn.[4] This feature leads to the conclusion that for large $N$, where $N$ is the number of bonds in a sequence in motion, the internal resistance is negligibly small compared to that of the environment.[4]

Long-wavelength motions are satisfactorily described on the basis of the diffusion equation of the Rouse–Zimm model.[5] Alternately, local jump stochastic models, where a master equation governs the time evolution of conformational transitions, have been used to treat chain dynamics.[6,7] In this latter approach, the slower normal modes of relaxation are shown to exhibit the Rouse chain behavior, while the high-frequency part of the spectrum is explicity influenced by local chain structure.[8] It is worth noting that the jump stochastic models have two shortcomings: first, the out-of-lattice effects are not included, and second, the external resistance to motion is considered only implicitly, through the transition probabilities.

The Brownian dynamics simulation technique is another useful tool for a clearer understanding of the mechanisms and rates of local conformational motions in polymers. In this approach the above mentioned two shortcomings are avoided. In an early Brownian motion study, Fixman[9] explored the effect of barrier heights and chain lengths on the rates of relaxational modes and on the decay with time of bond dihedral angle autocorrelations. Except for the longest wavelength modes, significant departure from Rouse-like rates is observed, the latter being stronger, for higher barriers to bond rotations. Also, the dependence of the rates on the number $N$ of bonds in the moving segment is found[9] to be weaker than that of the Rouse model in which the rates scale with $1/N^2$. In the limit as $N \to \infty$, a finite relaxational rate characteristic of single-bond torsional motion remains.[9] The latter is in reasonable agreement with the predictions of the Kramers theory.[10] That the local motions are activated by energies of about one barrier height between rotational isomeric minima and the applicability of the Kramers rate expression for rotameric transitions are also confirmed by the Brownian dynamics simulations by Helfand and collaborators.[11-14] More precisely, their work reveals that correlated or cooperative motions of type 2 where a bond rotation is immediately followed by a counterrotation of a second neighbor occur quite frequently. About 30% of conformational transitions belong to that group. However, the majority of conformational transitions occur by isolated single-bond rotations of the form $t \rightleftarrows g^{\pm}$.

Brownian dynamics simulations have the advantage of analyzing motions of relatively long chains. However, in the reported studies, a limited subset of conformational transitions has been considered only. On a local scale on the other hand, a model faithful to structural and conformational details of the real chain, incorporating the whole set of conformational transitions, is provided by the dynamic extension of the rotational isomeric state (DRIS) model.[15] The latter is however limited to a rather short sequence.

The DRIS model originates from an early work by Jernigan.[16] The same approach was later used by Beevers and Williams in the analysis of dielectric relaxation data.[17] The stochastics of conformational transitions were recently analyzed in a series of papers.[15,18-21] Calculations elucidate several aspects of local chain dynamics such as the experimentally observed[22] activation energies of about one barrier height in dilute solution,[18,21] the contribution of a family of internal orientational modes to relaxation leading to an OACF (orientational autocorrelation function) decay significantly different from a single exponential,[20] and the anisotropic nature of motions on the local scale.[19] The approach allows for a realistic estimation of the role of internal effects on local relaxational behavior provided that the external effect is eliminated by adopting a mean frictional resistance, regardless of the size of the reorienting unit. Calculations along this line confirm[15,16,20] the occurrence of an increase in "chain stiffness" accompanying the decrease in the size of the mobile group. In fact, longer sequences are found to relax faster, confirming the decrease in internal viscosity as $N$ increases, in parallel with Kuhn's[3,4] predictions. This behavior is attributed[15] to the increase in the number of degrees of freedom and hence in the number of allowable paths to relaxation in longer sequences. Recently, quantitative agreement with the spin–lattice relaxation times and correlation times from NMR experiments with polyethylene oxide in dilute solution was made possible by confining the DRIS analysis to a representative short segment of four bonds.[21]

The previous applications of the DRIS model have been confined to the consideration of internal effects associated with the barriers to conformational changes. However, chain dynamics is affected by other factors. For instance, the work of Skolnick and Helfand[23] shows that transitions in which the separation of the reorienting units from the axis of rotation is relatively small are easily accommodated by compensating fluctuations of the various degrees of freedom of the chain. Such distortions, among which the bond torsional angles are the softest, minimize the motion of the tails. They do not require high energy provided that they are spread over a large distance along the chain. This mechanism suggests that the resistance imposed by the tails on a mobile sequence is not strong enough to have a major influence on conformational stochastics.

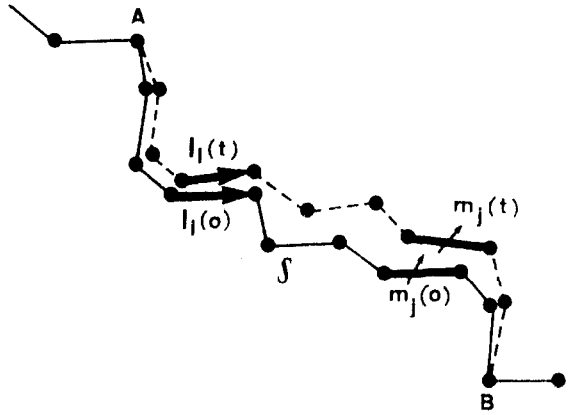


**Figure 1.** Contour **S** of the chain between points *A* and *B*. A rotameric transition in the *i*th bond changes the conformation of the contour from the solid line to the dashed line. The vector for the *i*th bond is shown as $\mathbf{l}_i(0)$ at time 0 and as $\mathbf{l}_i(t)$ at $t$. $\mathbf{m}_j(0)$ and $\mathbf{m}_j(t)$ denote the label $\mathbf{m}_j$, affixed to the *j*th bond at time $t = 0$ and $t$, respectively.

On the other hand, in previous studies using the DRIS model, the external effect arising from the frictional resistance of the environment was accounted for by a Stokes' type expression for the effective viscosity. Although an average effective solvent friction coefficient may be adopted for a given length of mobile segment, the relative contribution of various size segments to relaxation can not be understood unless a proper frictional resistance as a function of the volume swept during transition is incorporated into the treatment. In the present paper, we complement the previous DRIS formalism by including the effect of external resistance to motion. This effect is treated by considering the lengths of the paths traveled by the moving atoms during conformational transitions, within the Kramers-type rate expression[10] of the theory, similar to but in more detail than the work of Mashimo.[24] In addition to the treatment of internal orientational autocorrelations by DRIS, the influence of out-of-lattice compensating motions is independently explored.

## The Model and Assumptions

On the basis of the work by Helfand and collaborators,[1,12-14,23] where single bond rotations followed by compensating rearrangements of the neighboring units are predominantly responsible for local motions, the following model is proposed.

Figure 1 shows contour **S** between point *A* and *B* in a flexible chain, which undergoes an instantaneous jump from the configuration shown by the solid line to the one shown by the dashed line. We are interested in the orientation of a probe $\mathbf{m}_j$, located at the *j*th bond, within the mobile segment. We assume the following:

(a) The mobile segment belongs to an infinitely long chain (no end effects affect the motion).

(b) A single rotational transition takes place at a given time. In the figure, the transition takes place at the bond $\mathbf{l}_i$. Its isomeric state (trans, gauche$^+$, gauche$^-$)[2,5] is changed. This transition affects the orientation and the position of the label $\mathbf{m}_j$.

(c) The transition affects only a finite contour length **S** along the path on two sides of $\mathbf{l}_i$. The size of **S** may differ depending on the configurational transition. The requirement is that it should contain $\mathbf{m}_j$. The parts of the chain outside of **S** are referred to as the tails. A transition may take place without rearrangements of the tails (i.e., displacement or reorientation) if the bonds in **S** rearrange themselves to some extent, for example, by slight distortion of bond angles, bond lengths, and torsional angles, as in the treatment by Helfand and collaborators.

(d) The bond $\mathbf{l}_i$ will be both displaced and oriented during the rotational transition, as required for accommodating the transition over **S** without appreciably moving the tails. This type of compensating motion undergone by the transforming bond itself is implicitly present in the Brownian dynamics simulation by Helfand. The orientation of $\mathbf{m}_j$ obtained in this manner will be the resultant of an internal motion associated with the isomeric transition of the rotating bond $\mathbf{l}_i$ and the accompanying compensating motion. The extent of orientation of $\mathbf{m}_j$ resulting from the internal motion depends on the number and states of the bonds between $\mathbf{l}_i$ and $\mathbf{m}_j$.

(e) The motion induced by single-bond isomeric rotation depends on the configurational state of **S**. Inasmuch as a large number of different configurations of bonds in **S** will correspond to a given internal motion, the reorientation and displacement of $\mathbf{l}_i$ accompanying its torsion will be more or less random, i.e., independent of the given internal motion. Moreover the reorientation of $\mathbf{l}_i$ will be isotropic. Also, as the compensating motion is spread over a large length **S**, the change in the direction of $\mathbf{l}_i$ will be small. The calculations below will show that, in fact, a large number of configurational transitions are compatible with the requirement of preserving the tails of the sequence in motion approximately fixed, provided that the number of bonds in **S** is about 20 or higher.

(f) The bond $\mathbf{l}_i$ undergoing the transition may be either to the left or to the right of $\mathbf{m}_j$. Both locations are equivalent. In our model we assume that $\mathbf{l}_i$ is to the left of $\mathbf{m}_j$. For the evaluation of the internal dynamics of $\mathbf{m}_j$ relative to $\mathbf{l}_i$, the left-hand side of $\mathbf{l}_i$ is conventionally held fixed while the right-hand side rigidly follows the rotational motion. However, this approach overestimates the reorientation and displacement of $\mathbf{m}_j$ since the left-hand side need not be fixed and a given rotation of $\mathbf{l}_i$ will be evenly distributed at both sides of $\mathbf{l}_i$. Attention will be paid to this feature in analyzing the numerical results.

## Theory

A schematic representation of the orientational motion, according to the model delineated above, is shown in Figure 2. In agreement with assumption b, a single rotation over bond $\mathbf{l}_i$ is responsible for the motion. The latter is also displaced and reoriented with respect to a laboratory-fixed frame *XYZ*, following assumption d. $\mathbf{l}_i$ is assumed to coincide with the $\xi$-axis of a bond-based coordinate system $\xi\eta\zeta$, which moves with $\mathbf{l}_i$. The axes of the molecule-fixed coordinate system are denoted by $\xi(0)\eta(0)\zeta(0)$ at $t = 0$ and $\xi(t)\eta(t)\zeta(t)$ at $t$. $\mathbf{m}_j$ is the vector whose orientational motion is investigated. It is rigidly affixed to the *j*th bond, as indicated by the subscript *j*. The subscript *j* will be omitted in the following for brevity.

The vector **m** may be represented in the laboratory-fixed and the molecule-fixed coordinate systems at times zero and $t$ as follows:

$$\mathbf{m}(0) = \mu_\alpha(0)\epsilon_\alpha(0) = m_i(0)\mathbf{e}_i$$
$$\mathbf{m}(t) = \mu_\alpha(t)\epsilon_\alpha(t) = m_i(t)\mathbf{e}_i \quad (1)$$

Here $\mathbf{e}_i$ denote the base vectors along the coordinates *XYZ*. $\epsilon_\alpha(0)$ and $\epsilon_\alpha(t)$ are the base vectors along the coordinates $\xi(0)\eta(0)\zeta(0)$ and $\xi(t)\eta(t)\zeta(t)$, respectively. $\mu_\alpha$ and

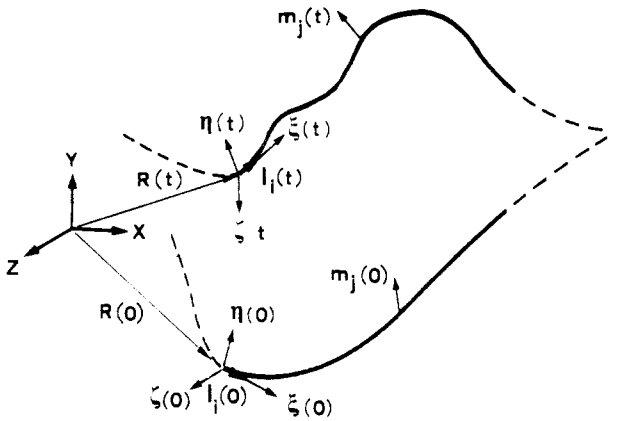


**Figure 2.** Displacement and rotation of label $\mathbf{m}_j$ on an isomeric transition in bond $j$. The bond vector $\mathbf{l}_i(0)$ changes into $\mathbf{l}_i(t)$ in order to accommodate the transition without appreciably moving the tails. $\xi(0)\eta(0)\zeta(0)$ and $\xi(t)\eta(t)\zeta(t)$ are the coordinate systems affixed to bond $\mathbf{l}_i$ at time 0 and $t$, respectively. $XYZ$ denotes the laboratory-fixed reference frame. $\mathbf{R}(0)$ and $\mathbf{R}(t)$ represent the position vector of $\mathbf{l}_i$ at $t = 0$ and $t$. The dashed curves are portions of the sequence leading to the tails.

$m_i$ denote the components of the vector $\mathbf{m}$ relative to molecule-fixed and laboratory-fixed systems, respectively. Summation is assumed over repeated indices. The orientational autocorrelation function (OACF), $\Phi_{ext}(t)$, for $\mathbf{m}$ as observed from the laboratory-fixed coordinate system is defined as

$$\begin{aligned}\Phi_{ext}(t) &= \langle \mathbf{m}(0)\cdot\mathbf{m}(t)\rangle \\ &= \langle \mu_\alpha(0)\mu_\beta(t)\epsilon_\alpha(0)\cdot\epsilon_\beta(t)\rangle \\ &\equiv \langle M_{\alpha\beta}(t)T_{\alpha\beta}(t)\rangle \end{aligned} \quad (2)$$

where the brackets denote the ensemble average over all configurations accessible to the segment. The second line follows from eq 1, and the elements of the matrices $M_{\alpha\beta}$ and $T_{\alpha\beta}$ are

$$M_{\alpha\beta}(t) = \mu_\alpha(0)\mu_\beta(t) \qquad T_{\alpha\beta}(t) = \epsilon_\alpha(0)\cdot\epsilon_\beta(t) \quad (3)$$

The components $M_{\alpha\beta}$ are obtained as the product of the components of $\mathbf{m}$ relative to the molecule-fixed reference frame. $T_{\alpha\beta}$ represents the transformation matrix from the system $\xi(0)\eta(0)\zeta(0)$ to $\xi(t)\eta(t)\zeta(t)$ and hence reflects the effect of the compensating motions on the OACF. By use of assumption e, of the independence of internal and compensating motions, eq 2 is written as

$$\Phi_{ext}(t) = \langle M_{\alpha\beta}(t)\rangle\langle T_{\alpha\beta}(t)\rangle \quad (4)$$

For small rotations, the off-diagonal terms of $\langle T_{\alpha\beta}(t)\rangle$ will be small compared to the diagonal elements. Also following the assumption of isotropic compensating motion, the three diagonal elements of $\langle T_{\alpha\beta}(t)\rangle$ will be approximately equal to each other. Denoting the latter by $T_{11}(t)$, eq 4 reduces to

$$\begin{aligned}\Phi_{ext}(t) &= \langle T_{11}(t)\rangle\langle M_{11}(t) + M_{22}(t) + M_{33}(t)\rangle \\ &\equiv \langle T_{11}(t)\rangle\Phi_{int}(t) \end{aligned} \quad (5)$$

Here the second line follows from the definition of the OACF, where $\Phi_{int}(t)$ represents the OACF of $\mathbf{m}(t)$ as observed from the molecule-fixed coordinate system. Equation 5 is of fundamental importance. It shows that, under the assumptions clearly set forth above, the orientational autocorrelation function for vector $\mathbf{m}$ may be expressed as the product of an internal and external OACF. This was in fact suggested several years ago by Stockmayer et al.[8] who introduced the rotational diffusion of the overall segment as a second fundamental dissipative process in parallel to local conformational flips.

The internal OACF has been the subject of a series of studies in which the direction and location of the rotating bond were kept fixed in space. The incorporation of compensating dynamics into them is achieved simply by multiplying with an average cosine of the reorientation of the rotating bond. $\langle T_{11}(t)\rangle$ is expected to decay as a single exponential. Indeed, it reflects the effect of the out-of-lattice fluctuations on the orientational motion, for which a single-exponential decay has been previously proposed.[26]

**Internal Motions. DRIS Approach.** The stochastics of conformational transitions is fully described by the transition probability matrix $\mathbf{C}$ whose $IJ$th element $C_{IJ}$ represents the time-dependent probability of transition from the initial configuration $\{\phi\}_J$ to the final one $\{\phi\}_I$. Here capital indices $I$ and $J$ are employed for the configurations, to distinguish them from the bond indices $i$, $j$, etc. Clearly, each configuration characterized by the set of $N$ isomeric states associated with the backbone bonds $\mathbf{C}$ obeys the master equation[15]

$$d\mathbf{C}/dt = \mathbf{AC} \quad (6)$$

where $\mathbf{A}$ is the matrix of the rate constants.[15,18-21] Its element $A_{IJ}$, with $I \neq J$, represents the rate constant for the passage from the $J$th configuration to the $I$th one. If those configurations possess more than one bond, differing in state, $A_{IJ}$ equates to zero, following assumption b of single bond rotation at a time stated above. Otherwise $A_{IJ}$ is given by

$$A_{IJ} = \begin{cases} A_0 \exp\{-E_i/RT\} & \text{for } I \neq J \\ -\sum_{K\neq J} A_{KJ} & \text{for } I = J \end{cases} \quad (7)$$

Here $R$ is the gas constant and $T$ is the absolute temperature. The activation energy $E_i$ is determined from the height of the energy barrier surmounted by the single rotating bond $i$ during its isomeric transition. Two-dimensional energy surfaces based on the pairwise dependence of consecutive torsional angles have been used in previous work to estimate $E_i$.[15,18-21] The latter is an inherent characteristic of the polymer chain in question regardless of its state (i.e., in bulk or in solution). It will always contribute to the apparent activation energy.

The front factor in eq 7 is taken as

$$A_0 = (\gamma\gamma^*)^{1/2}/(2\pi\zeta\sum_{j=i+1}^{N} s_{ij}^2) \quad (8)$$

where $\gamma$ and $\gamma^*$ refer to the curvature of the energy path at the minimum and maximum, respectively, assuming the prevailing potential to be of the form $U = (1/2)\gamma(\phi - \phi_{min})^2$ at the minimum and $U = (1/2)\gamma^*(\phi - \phi_{max})^2$ at the maximum. $\phi$ is the torsional angle of the rotating bond; $\phi_{min}$ and $\phi_{max}$ are the values at the isomeric minimum and at the top of barrier, respectively. $\zeta$ is the friction coefficient. As shown in Figure 3, $s_{ij}$ represents the separation of the $j$th atom from the axis of rotation, which is defined by the rotating bond $i$. It is assumed that bond $i$ connects the atoms $i-1$ and $i$, following usual convention. Its transition sets in motion the neighboring $N$ atoms with indices $i + 1 \leq j \leq N$. Inasmuch as conformational transitions from one isomeric state to another involve about 120° bond rotations, the path traveled by the moving atom is approximately equal to $s_{ij}$. Thus the term $\sum_{j=i+1}^{N} s_{ij}^2$ in eq 8 is representative of the total squared distance swept by the ensemble of those

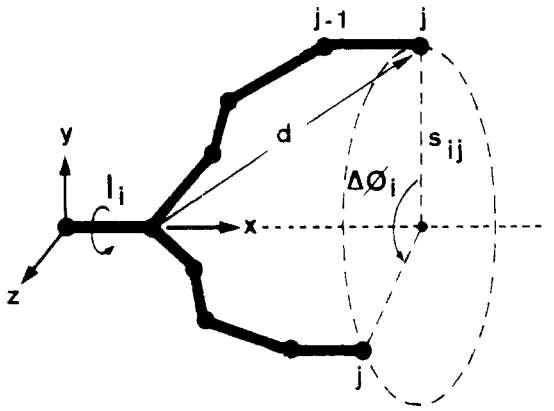


**Figure 3.** Displacement of the $j$th atom due to a rotation over the $i$th bond, $s_{ij}$ is the distance from the axis of rotation to the $j$th atom. $\Delta\phi_i$ represents the rotation about $\mathbf{l}_i$.

atoms accompanying the isomeric transition of bond $i$.

The introduction of the term $\sum s_{ij}^2$ in the denominator of the front factor $A_0$ accounts for the frictional resistance exerted by the environment to the reorientation of the sequence. The latter leads to a considerable slowing down of the motion as $N$ increases. This effect will be referred to as the size effect and calculations will be performed for the two cases: (i) using eq 8 coupled with eq 7, i.e., assigning a distinct rate to each transition depending on the path traveled by the mobile atoms; (ii) ignoring the size effect and adopting a mean value $s^2$ instead of $\sum s_{ij}^2$ for all rates regardless of the number of bonds in motion. The latter approach was adopted in previous studies[15,18-21] and reflects the influence of the internal resistance only. Repeating the calculations for the two cases (see sequel) will explicitly give information on the influence of the external resistance on local motions.

For a bond vector subject to the rotational motion of the $N$ preceding bonds the correlation time is calculated from[21]

$$\tau = -(1 - k_1)^{-1} \sum_{j=2}^{3^N} k_j/\lambda_j \tag{9}$$

with

$$k_j = \sum_i \sum_n B_{ij} B_{jn}^{-1} P_n^0 [3(\mathbf{m}_i \cdot \mathbf{m}_n) - 1]/2 \tag{10}$$

where $\lambda_j$ is the $j$th eigenvalue of $\mathbf{A}$, $P_n^0$ is the equilibrium probability of the initial configuration $\{\phi\}_n$, $\mathbf{m}_i$ is the vectorial representation of the bond of interest when the sequence assumes the configuration $\{\phi\}_i$ at time $t$, and $B_{ij}$ and $B_{jn}^{-1}$ are elements of $\mathbf{B}$ and its inverse $\mathbf{B}^{-1}$, which are found from the similarity transformation $\mathbf{A} = \mathbf{B}\Lambda\mathbf{B}^{-1}$, $\Lambda$ being the diagonal matrix of the eigenvalues. $k_j$ represents the a priori probability of relaxation through internal mode $j$ with frequency $\lambda_j$. $k_1$ corresponds to the zero eigenvalue $\lambda_1$.

Equation 9 directly follows from the definition[27]

$$\tau = \int_0^\infty (\Phi(t) - \Phi(\infty))/(\Phi(0) - \Phi(\infty))\, dt \tag{11}$$

for the correlation time, in which the OACF $\Phi(t)$ given by[21]

$$\Phi(t) = \sum_j k_j \exp\{\lambda_j t\} \tag{12}$$

is substituted. In general $k_j$ assumes different forms depending on the investigated correlations. The expression given by eq 10 is for the second OACF.

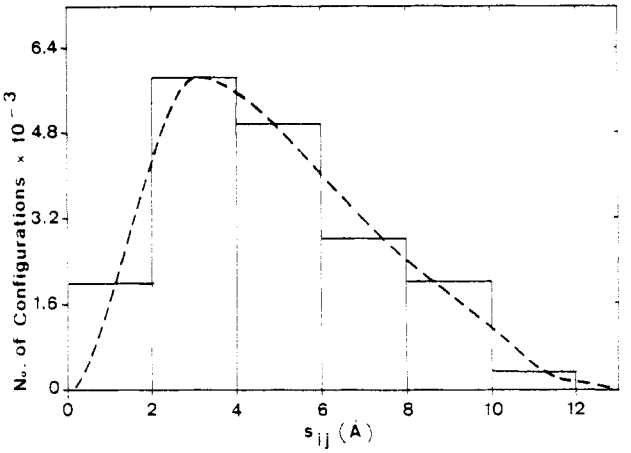


**Figure 4.** Number of configuration corresponding to a given value of $s_{ij}$. Intervals of 2 Å are chosen for $s_{ij}$ in obtaining the ordinate values.

Equation 9 represents nothing other than the weighted average of the relaxation times associated with each individual mode. As a consequence the slowest modes dominate the resulting correlation time. On the other hand, if short time intervals are of interest, the definition

$$\tau = -(1 - k_1)/\sum_j k_j \lambda_j \tag{13}$$

may be preferred over eq 9. $\tau$ given by eq 13 represents the intersection of the initial tangent to the OACF decay curve with the $\Phi(t) = k_1$ asymptote. According to eq 13, the various relaxational frequencies $|\lambda_j|$ contribute additively to yield a correlation time shorter than the one implied by eq 9. Both definitions (eqs 9 and 13) will be considered and discussed in the following quantitative analysis of correlation times.

## Calculations

**Long-Range Effect of Connectivity.** To estimate the strength of the constraint imposed by the tails on local motions, we consider a portion of a hypothetical, perfect tetrahedral chain with three equally probable states (t, $g^+$, $g^-$) available to each bond. A change in configuration is made by rotating the central bond $\mathbf{l}_i$ by a torsional angle of $\Delta\phi = \pm 120°$. This rotation is propagated along both sides of the mobile bond, as mentioned in the model. For a quantitative evaluation of the displacement of the tails accompanying the rotation, let us consider a segment of about 20 bonds with bond $\mathbf{l}_i$ in the middle. For simplicity let us assume first that the left-hand side is fixed and the rotation moves the right-hand side of $\mathbf{l}_i$ only. Let us examine the displacement of the 11th atom $j$ from atom $i$. The displacement undergone by atom $j$ will depend on the isomeric states of the nine intermediate bonds between atoms $i + 1$ and $j - 1$. Atom $j$ will be displaced along a 120° arc on the circle with radius $s_{ij}$ (see Figure 3). The distribution of $s_{ij}$ is shown in Figure 4. The latter is found from the complete enumeration of the $3^9$ configurations. The quoted numbers in the ordinate refer to the number of configurations corresponding to $s_{ij}$ intervals of 2 Å. The dashed curve is drawn to guide the eye. Bond lengths are taken as 1.53 Å.

Let us assume that the 11th atom from the mobile bond undergoes a displacement less than 4 Å. From the distribution above, the subset of chains satisfyings this requirement amounts to 41% of the total ensemble. Considering that the left-hand side of $\mathbf{l}_i$ will also be moving,

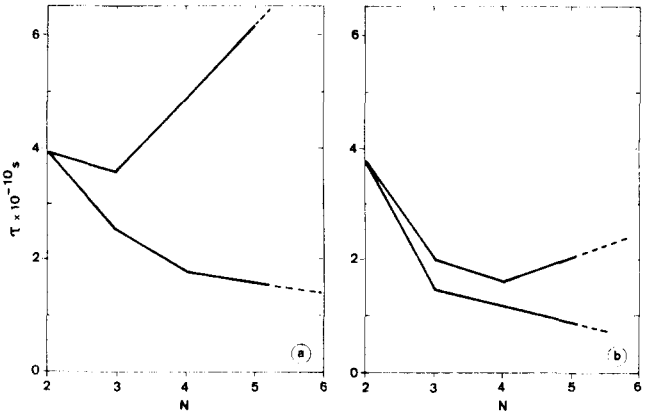


**Figure 5.** Variation of correlation times $\tau$ with the number of bonds in the mobile unit: (a) from eq 9; (b) from eq 13. In both parts, the lower curves are obtained without the size effect and the upper curves with the size effect.

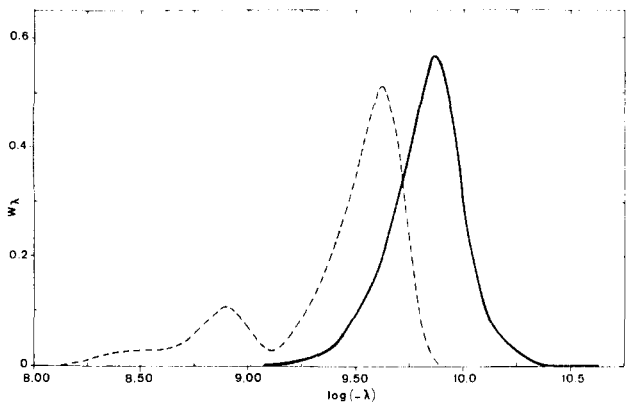


**Figure 6.** Frequency distribution of internal relaxational modes in a sequence of four mobile bonds in PE at 300 K. The solid and dashed curves are obtained without and with the size effect, respectively.

this displacement will be spread over the 22 bonds, effectively leading to a displacement of 2 Å for each end. Such a displacement is sufficiently small to be easily accommodated by the compensating motions mentioned above. Thus, the restriction of confinement of the tails within a small volume is not as severe as conceived. If an additional constraint, that of the change in the orientation of the last bond (here $\mathbf{l}_{j-1}$), is considered, then the number of allowable transitions is further reduced. For example, let us assume that in the segment of 21 bonds, the orientation of the two terminal bonds changes each by less than 15°. Then among the total of $3^{18}$ configurations, $(2138)^2$ transitions are computed to succeed in meeting the two above spatial and directional requirements. Thus the central bond $\mathbf{l}_i$ may undergo any of the six isomeric transitions between the state t, $g^+$, and $g^-$ if the neighboring bonds undergo one of those $(2138)^2$ transitions.

Let $\alpha$ denote the angular displacement of the end-to-end vector $\mathbf{l}_i + \mathbf{d}$ in Figure 3, during the conformational transition. Calculations holding the left-hand side of $\mathbf{l}_i$ fixed yield $\langle \cos^2 \alpha \rangle = 0.435$, for the final subset of allowable transitions. Inasmuch as the change in orientation is distributed over both sides of $\mathbf{l}_i$, an average angular displacement of about 24° is estimated for the segment of 20 bonds. Such an angular motion may easily be accommodated by about 2° angular distortions (torsional or bending) of the bonds flanking $\mathbf{l}_i$. Moreover the suitable translation of bond $\mathbf{l}_i$ may further help to minimize the constraints imposed by the tails. Thus, the analysis above clearly demonstrates that long-range connectivity is of secondary importance in dictating the stochastics of local conformational transitions.

**Dependence of Orientational Correlation Times on Size Effect.** Calculations are performed for different sizes of mobile sequences in polyethylene chain at 300 K. The same parameters as those employed previously[15] are adopted. The resulting correlation times associated with the orientational motion of a vector $\mathbf{m}$ are shown in Figure 5 as a function of $N$. The investigated vector $\mathbf{m}$ is affixed along the $N$th bond of a sequence whose first bond in kept fixed in space. Thus, compensating motions of the mobile sequence are not included in the calculations. The obtained correlation times are representative of the internal dynamics only.

The curves in Figure 5a are obtained by using eq 9. The upper and lower curves correspond to dynamics in the presence and absence of a size effect, respectively. The equivalent curves following from the definition of $\tau$ given by eq 13 are shown in Figure 5b. It should be recalled that the former definition is representative of motions observed in a large time window while the latter is applicable to experiments probing relative high frequency motions. In fact, the correlation times predicted by eq 13 in Figure 5b are lower than those resulting from eq 9 in Figure 5a. In both figures the lower curves are found by adopting a mean value $s^2 = l^2 \sin^2 \theta$ where $l = 1.53$ Å and $\theta = 68°$, instead of $\sum_j s_{ij}^2$ of eq 8, regardless of the number of moving atoms and their respective displacements. Inasmuch as the front factor is kept constant, the variation of $\tau$ with $N$ indicates the contribution to relaxation from internal barriers uniquely and shows the internal stiffening caused by a decrease in $N$. It is worth noting that in this case $\tau$ is proportional to $1/N$ at larger values of $N$. However, this internal stiffening is more than counter balanced by the size effect, with increasing $N$, as may be observed from the upper curves in Figure 5a,b. In this case, a minimum is observed for $N = 3$ (Figure 5a) and $N = 4$ (Figure 5b), depending on the definition of $\tau$. It is interesting to note that a similar minimum was found at short wavelengths by Allegra[28] in his analysis of Langevin dynamics including friction effects on each atom.

Figure 6 shows the frequency distribution of internal relaxational modes over the range $10^8 < |\lambda| < 10^{11}$ s$^{-1}$, in a sequence of four mobile bonds in PE at 300 K. The solid and dashed curves are obtained without and with the size effect, respectively. The ordinate $W_\lambda$ is found by summing the $k_j$ values corresponding to the eigenvalues lying in intervals of $\Delta \log(-\lambda) = 0.25$. It is interesting to note that the frequency distribution is not significantly perturbed by including the size effect. The main result of the latter is a common shifting of the frequencies to lower values, although a small new peak also appears at lower frequencies. The friction coefficient $\zeta$ is held constant in the calculations and does not contribute to the shift of the spectrum shown in Figure 6. Thus the shift in the spectrum is characteristic of the number of bonds in the mobile sequence.

## Discussion

In this paper, we have complemented the previous work based on the DRIS approach by considering two important aspects of local chain dynamics: the chain connectivity and the size effect.

In relation to the effect of chain connectivity, the present calculations indicate that for a sufficiently long sequence (~20 bonds) a large number (~$4 \times 10^6$) of conforma-

tional transitions induced by single-bond rotations are possible without appreciably moving the ends of the mobile sequence. Furthermore, the constraints imposed by chain connectivity may be reduced by spreading the resulting rotational and translational displacements over the neighboring units as considered by Helfand and co-workers. From Brownian dynamics simulations, Fixman also concludes that the so-called chain effect arising from the connected neighboring units does not have a significant effect on local dynamics, although in his approach, in contrast to Helfand, the cooperative compensating effects are not considered.

The size effect refers to the increase in the frictional resistance to motion with the number of moving atoms and the length of their displacements. Calculations where a mean viscous resistance was adopted regardless of the size of the orienting unit reflect the contribution of internal barriers to local motion. They lead to correlation times proportional to $1/N$, in qualitative agreement with the so-called internal viscosity effect, pointed out by Kuhn.[4] When the size effect is considered, it is shown that the $N$ dependence of $\tau$ is inverted above $N = 3$ or 4. The implications of the above analysis at large $N$ would be of interest in comparison to previous work. Fixman's Langevin dynamics simulations demonstrate that the relaxation rates converge to a finite value at large $N$. Also, the analytical treatment of conformational kinetics by Skolnick and Helfand and the Brownian motion simulations by Helfand and collaborators show that the motion of a central bond becomes insensitive to the length of the tails beyond a certain value of $N$. The asymptotic value to which $\tau$ converges as $N \rightarrow \infty$, according to the present work, depends on the definition (eq 9 or 13) adopted for $\tau$.

The expression for $\tau$ according to eq 9 consists of the sum of $3^N - 1$ terms. Each term varies inversely with an eigenvalue, $\lambda_j$. Slowing down of the motions by introducing the expression $\sum_j s_{ij}^2$ in the denominator of the front factor is directly reflected on each $\lambda_j$. Consequently, a set of $\lambda_j$'s will necessarily vanish as $N$ increases indefinitely. This leads to an infinite $\tau$ according to eq 9.

Equation 13 on the other hand associates $\tau$ with the incipient rate of relaxation. In this case, the set of $\lambda_j$'s going to zero with increasing $N$ will not contribute to the correlation time and $\tau$ will converge to a finite value, at large $N$. This behavior following from the definition of $\tau$ as the inverse of the incipient rate of relaxation is in conformity with the simulations carried out by Fixman. It is worth noting that the ambiguity in defining the correlation time arises from the presence of a distribution of modes. Indeed for systems with a single mode, the two definitions of $\tau$ given above by eqs 9 and 13 are equivalent.

**Acknowledgment.** This work was supported by NATO Grant 0321/87 and by the French Ministère de la Recherche et de la Technologie.

## References and Notes

(1) Helfand, E. *J. Chem. Phys.* **1971**, *54*, 4651.
(2) Boyer, R. F. *Rubber Chem. Technol.* **1963**, *34*, 1303. Schatzki, T. F. *J. Polym. Sci.* **1962**, *57*, 496; *Polymer Prepr. (Am. Chem. Soc., Div. Polym. Chem.)* **1965**. Valeur, B.; Jarry, J.-P.; Gény, F.; Monnerie, L. *J. Polym. Sci., Polym. Phys. Ed.* **1975**, *13*, 667.
(3) de Gennes, P.-G. *Scaling Concepts in Polymer Physics*; Cornell University Press: Ithaca, NY, 1979.
(4) Kuhn, W.; Kuhn, H. *Helv. Chim. Acta* **1945**, *28*, 1533; **1946**, *29*, 7, 609, 830.
(5) Rouse, P. E. *J. Chem. Phys.* **1953**, *21*. Zimm, B. H. *J. Chem. Phys.* **1956**, *24*, 269.
(6) Orwoll, R. A.; Stockmayer, W. H. In *Stochastic Processes in Chemical Physics*; Schuler, K. E., Ed.; *Adv. Chem. Phys.* **1969**, *15*, 305.
(7) Valeur, B.; Jarry, J. P.; Gény, F.; Monnerie, L. *J. Polym. Sci., Polym. Ed.* **1975**, *13*, 667.
(8) Stockmayer, W. H.; Gobush, W.; Chikahisa, Y.; Carpenter, D. K. *Faraday Discuss.* **1970**, *49*, 182.
(9) Fixman, M. *J. Chem. Phys.* **1978**, *69*, 1527, 1538.
(10) Kramers, H. A. *Physica* **1940**, *7*, 284.
(11) Helfand, E. *Science* **1984**, *226*, 647.
(12) Helfand, E. *J. Chem. Phys.* **1978**, *69*, 1010.
(13) Helfand, E.; Wasserman, Z. R.; Weber, T. A. *Macromolecules* **1980**, *13*, 526.
(14) Helfand, E.; Wasserman, Z. R.; Weber, T. A. *J. Chem. Phys.* **1979**, *70*, 2016.
(15) Bahar, I.; Erman, B. *Macromolecules* **1987**, *20*, 1368.
(16) Jernigan, R. L. In *Dielectric Properties of Polymers*; Karasz, F. E., Ed.; Plenum: New York, 1972; p 99.
(17) Beevers, M. S.; Williams, G. *Adv. Mol. Relax. Proc.* **1975**, *7*, 237.
(18) Bahar, I.; Erman, B. *Macromolecules* **1987**, *20*, 2310.
(19) Bahar, I.; Erman, B. *J. Chem. Phys.* **1988**, *88*, 1228.
(20) Bahar, I.; Erman, B.; Monnerie, L. *Macromolecules* **1989**, *22*, 431.
(21) Bahar, I.; Erman, B.; Monnerie, L. *Polym. Commun.* **1988**. Bahar, I.; Erman, B.; Monnerie, L. *Macromolecules* **1989**, *22*, 2396.
(22) Baysal, B.; Lowry, B. A.; Yu, H.; Stockmayer, W. H. In *Dielectric Properties of Polymers*; Karasz, F. E., Ed.; Plenum: New York, 1972. Jones, A. A.; Matsuo, K.; Kuhlmann, K. F.; Gény, F.; Stockmayer, W. H. *Polym. Prepr.* **1975**, *16*, 578. Morawetz, H. *Science* **1979**, *203*, 405. Chen, D. T.-L.; Morawetz, H. *Macromolecules* **1976**, *9*, 463.
(23) Skolnick, J.; Helfand, E. *J. Chem. Phys.* **1980**, *72*, 5489. Helfand, E.; Skolnick, J. *J. Chem. Phys.* **1982**, *77*, 5714.
(24) Mashimo, S. *Macromolecules* **1976**, *9*, 91. Mashimo, S. *J. Polym. Sci., Polym. Phys. Ed.* **1981**, *19*, 213.
(25) Flory, P. J. *Statistical Mechanics of Chain Molecules*; Interscience: New York, 1969.
(26) Dubois-Violette, E.; Gény, F.; Monnerie, L.; Parodi, O. *J. Chim. Phys.* **1969**, *66*, 1865.
(27) Berne, B. J.; Pecora, R. *Dynamic Light Scattering with Applications to Chemistry, Biology and Physics*; Wiley Interscience: New York, 1976.
(28) Allegra, G. *J. Chem. Phys.* **1974**, *61*, 4910; **1978**, *68*, 3600.
(29) Kloczkowski, A.; Mark, J. E.; Bahar, I.; Erman, B., unpublished results.

**Registry No.** Polyethylene, 9002-88-4.